

Inactivation of SMC2 shows a synergistic lethal response in *MYCN*-amplified neuroblastoma cells

Yuko Murakami-Tonami^{1,†,*}, Satoshi Kishida¹, Ichiro Takeuchi², Yuki Katou³, John M Maris⁴, Hitoshi Ichikawa⁵, Yutaka Kondo^{6,7}, Yoshitaka Sekido⁶, Katsuhiko Shirahige³, Hiroshi Murakami⁸, and Kenji Kadomatsu^{1,*}

¹Department of Molecular Biology; Nagoya University Graduate School of Medicine; Nagoya, Japan; ²Department of Computer Science/Scientific and Engineering Simulation; Nagoya Institute of Technology; Nagoya, Japan; ³Laboratory of Genome Structure & Function; Institute of Molecular and Cellular Biosciences; The University of Tokyo; Tokyo, Japan; ⁴Department of Pediatrics and Center for Childhood Cancer Research; Children's Hospital of Philadelphia; University of Pennsylvania; Philadelphia, PA USA; ⁵Division of Genetics; National Cancer Institute; Tokyo, Japan; ⁶Division of Molecular Oncology; Aichi Cancer Center Research Institute; Nagoya, Japan; ⁷Division of Epigenomics; Aichi Cancer Center Research Institute; Nagoya, Japan; ⁸Department of Biological Science; Faculty of Science and Engineering; Chuo University; Tokyo, Japan

[†]Current affiliation: Aichi Cancer Center Research Institute; Division of Molecular Oncology; Kanokoden, Chikusa-ku Nagoya, Japan

Keywords: condensin complex, DNA damage response, *MYCN*, neuroblastoma, synergistic lethal response

The condensin complex is required for chromosome condensation during mitosis; however, the role of this complex during interphase is unclear. Neuroblastoma is the most common extracranial solid tumor of childhood, and it is often lethal. In human neuroblastoma, *MYCN* gene amplification is correlated with poor prognosis. This study demonstrates that the gene encoding the condensin complex subunit SMC2 is transcriptionally regulated by *MYCN*. SMC2 also transcriptionally regulates DNA damage response genes in cooperation with *MYCN*. Downregulation of *SMC2* induced DNA damage and showed a synergistic lethal response in *MYCN*-amplified/overexpression cells, leading to apoptosis in human neuroblastoma cells. Finally, this study found that patients bearing *MYCN*-amplified tumors showed improved survival when *SMC2* expression was low. These results identify novel functions of SMC2 in DNA damage response, and we propose that SMC2 (or the condensin complex) is a novel molecular target for the treatment of *MYCN*-amplified neuroblastoma.

Introduction

The condensin complex, which is highly conserved from bacteria to humans, is essential for proper chromosome condensation and segregation during mitosis and meiosis. There are 2 condensin complexes in human, condensin I and condensin II. These complexes share 2 common core subunits, SMC2/CAP-E and SMC4/CAP-C, and have 3 unique non-SMC subunits. Condensin I contains CAP-D2, CAP-H, and CAP-G, while condensin II contains CAP-D3, CAP-H2, and CAP-G2.¹

It has recently been reported that the condensin complex also has a number of functions during interphase, including DNA repair and transcriptional regulation. Human condensin I is required for the recruitment of PARP-1 to single-strand DNA breaks in HeLa and 293T cells.² In fission yeast, Cnd2 (human CAP-H), which is the non-SMC subunit of condensin, is synthetic lethal with the DNA replication protein RecQ helicase (human WRN, BLM and RecQL proteins) and is required for Cds1 (human CHK2) activation.³ Furthermore, the fission yeast SMC2 homolog Cut14 is required for DNA annealing.⁴ Human CAP-G2 is involved in the transcriptional regulation of *c-kit* in erythroid cells via an interaction with an erythroid-lineage-specific bHLH transcription factor.⁵ In addition, a genome-wide

analysis of budding yeast revealed that the chromosomal condensin pattern does not alter during the cell cycle, and that the minimal condensin-binding consensus comprises a B-box element recognized by RNA polymerase III transcription factor.⁶

Although a condensin knockout mouse model is currently unavailable,¹ knockdown of *Smc2* induces cell death in mouse embryonic stem cells but not in immortalized mouse embryonic fibroblasts.⁷ These findings suggest that the condensin complex is not essential for viability and may be differentially regulated across tissues or during development.

The MYC family of proteins comprises MYC (*c-myc*), *MYCN*, and MYCL. *MYCN* encodes a transcription factor with a β -helix-loop-helix domain that is specifically expressed in neuronal tissues. Multiple target genes are regulated by MYC, including DNA damage response (DDR) genes.^{8–12} Cancer cells undergo many stresses, including oxidative and replicative stress.¹³ According to the oncogene-induced DNA damage model of cancer development,¹⁴ genomic instability is induced by oncogenes themselves. In fact, MYC induces DNA damage through reactive oxygen species (ROS) production¹⁵ and replicative stress.¹⁶

The DDR is a network of signaling pathways involved in DNA damage repair, cell cycle checkpoints, and apoptosis.¹⁷ The

*Correspondence to: Yuko Murakami-Tonami; Email: ytona@aichi-cc.jp; Kenji Kadomatsu; Email: kkadoma@med.nagoya-u.ac.jp
Submitted: 01/13/2014; Accepted: 01/23/2014; Published Online: 02/07/2014
<http://dx.doi.org/10.4161/cc.27983>

MRN complex has been implicated in all aspects of DNA double-strand break (DSB) processing, including initial detection, triggering signaling pathways, and facilitating repair. The MRN complex also activates ataxia-telangiectasia mutated (ATM) and related kinases that promote rapid phosphorylation of multiple

proteins and of chromatin structure around the break sites. The 2 major DSB repair pathways are homologous recombination and non-homologous end-joining (NHEJ).¹⁸ BRCA1 is a versatile protein that links DNA damage sensing and DDR effectors. This protein is directly involved in homologous recombination-mediated repair of DSBs and may also function in other DNA repair pathways, including NHEJ and single-strand annealing.

Inhibiting genes that are synthetic lethal with cancer-associated mutations should exclusively kill cancer cells; therefore, identification of such genes is important for identifying new therapeutic targets.¹⁹ One of the most well-characterized therapeutic combinations comprises a *BRCA1* mutation and a poly-ADP-ribose polymerase inhibitor.^{20,21} To date, multiple specific combinations of genes have been found to show synergistic lethal responses with *MYC* or *MYCN*.²²⁻³¹

Neuroblastoma originates from precursor cells of the sympathetic nervous system. *MYCN* oncogene amplification and mutations in the gene encoding anaplastic lymphoma kinase (ALK) are both critically involved in the development of a high-risk clinical phenotype and poor survival probabilities.³²⁻³⁶ There are several animal models of neuroblastoma, including *MYCN* and mutated *ALK* transgenic mice.³⁷ *MYCN* transgenic (Tg) mice, in which *MYCN* expression is targeted to the sympathetic neuron lineage by rat tyrosine hydroxylase,³⁸ serve as a model of neuroblastoma. These mice develop aggressive neuroblastomas and tumorigenesis, positively correlated with the *MYCN* transgene dosage or the development of additional genetic mutations.³⁹

Here, we show that *SMC2* regulates several DDR genes in cooperation with *MYCN*, and that knockdown of *SMC2* has a synergistic lethal effect with *MYCN* amplification. *SMC2* controls several DDR genes simultaneously; therefore, it may be an effective molecular target for the treatment of *MYCN*-amplified cancers. In addition, we show that patients bearing *MYCN*-amplified tumors tend to benefit from low *SMC2* expression. The results presented here suggest that *SMC2* (or the condensin complex) is a molecular target of *MYCN*-amplified cancers.

Results

Smc2 expression in neuroblastoma model mice and human neuroblastoma cell lines

To gain insights into the molecular pathways governing neuroblastoma development, the expression profiles of superior mesenteric ganglia of 2-wk-old wild-type (wt) mice, precancerous lesions of 2-wk-old homozygote *MYCN* Tg mice, and terminal tumors of 6-wk-old homozygote *MYCN* Tg mice were examined (GSE43419). The expression levels of 79 genes were higher in precancerous lesions and tumors of *MYCN* Tg mice than in ganglia of wt mice. Among these genes, *Smc2* was selected and characterized further. The level of *Smc2* expression gradually increased as the severity of the disease progressed (Fig. 1A). To confirm this finding, semi-quantitative and quantitative RT-PCR (RT-qPCR) analyses of precancerous lesions of 2-wk-old *MYCN* hemizygous mice were performed (Fig. 1B); these lesions are reportedly similar to human *MYCN*-amplified

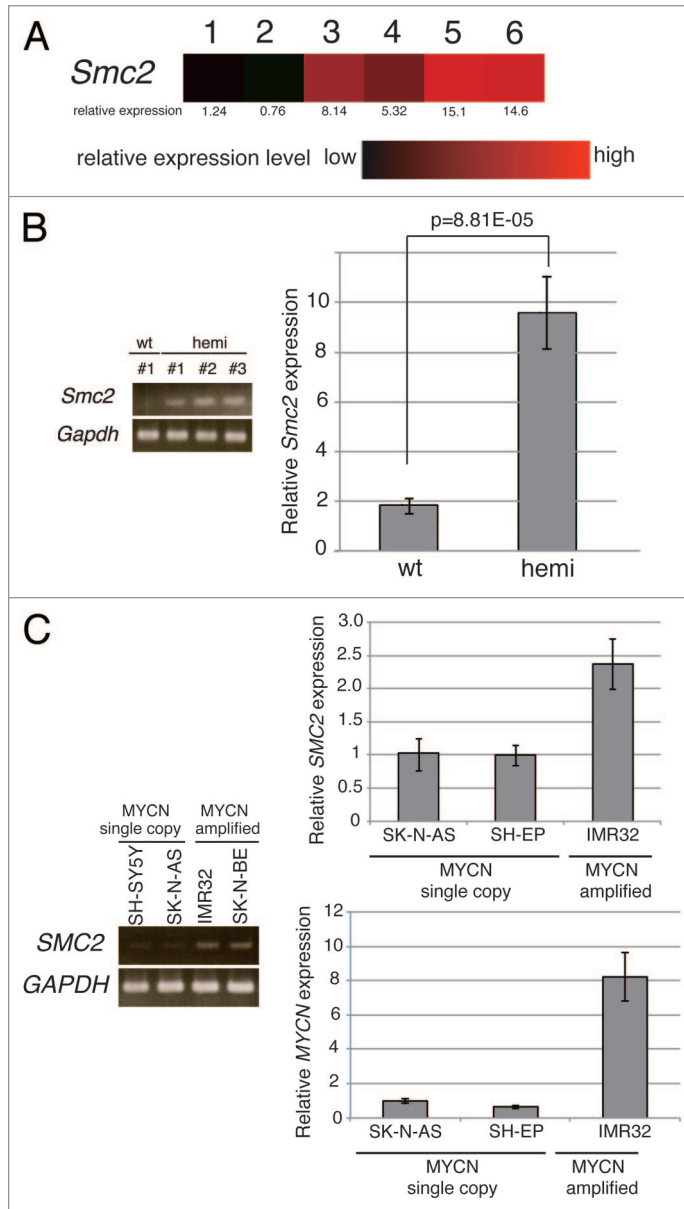


Figure 1. *Smc2* expression in neuroblastoma model mice and *SMC2* expression in human neuroblastoma cell lines. (A) Results of a microarray analysis of the relative expression levels of *Smc2* in ganglia of wt mice (lanes 1 and 2), and precancerous (lanes 3 and 4) and tumor lesions (lanes 5 and 6) of homozygous *MYCN* Tg mice. (B) Semi-quantitative (left) and quantitative (right) RT-PCR analyses of *Smc2* and *Gapdh* (control) expression levels in 3 precancerous lesion samples from hemizygous *MYCN* Tg mice (hemi) and ganglia of wt mouse. (C) Semi-quantitative (left) and quantitative (right) RT-PCR analyses of human *SMC2* expression levels in various human neuroblastoma cell lines. SH-SY5Y, SK-N-AS, and SH-EP cells have a single copy of *MYCN*, and IMR32 and SK-N-BE(2) have amplified *MYCN*. The expression levels of *Smc2* and *SMC2* detected by RT-qPCR were normalized to those of *Gapdh* and *GAPDH* respectively.

neuroblastoma.³⁹ Consistent with the microarray data, mouse *Smc2* was highly expressed in the precancerous lesion samples (Fig. 1B).

The expression of *SMC2* was then examined in human neuroblastoma cell lines. Human *SMC2* expression was higher in *MYCN*-amplified cell lines (IMR32 and SK-N-BE[2]) than in *MYCN* single copy cell lines (SH-SY5Y, SK-N-AS and SH-EP) (Fig. 1C). These results indicate that *SMC2* expression is elevated in *MYCN*Tg mice and *MYCN*-amplified human neuroblastoma cells and is correlated with *MYCN* expression.

Overexpression of MYCN induces SMC2 expression in human neuroblastoma cells

To determine whether overexpression of *MYCN* induces *SMC2* expression, a CMV-driven *MYCN* plasmid or a CMV-Venus

plasmid (as a control) were introduced into SH-EP *MYCN* single copy cells using a lentivirus. After live cell sorting, RT-PCR and immunoblotting analyses were performed. The levels of *SMC2* mRNA and protein were higher in SH-EP cells constitutively expressing *MYCN* than in control cells (Fig. 2A and B).

MYC binds to a canonical consensus DNA sequence (CACGTG) named the E-box. *MYC* also binds to several other non-canonical DNA motifs in vitro, including CATGTG, CATGCG, CACGCG, CACGAG, and CAACGTG.⁴⁰ Three canonical E-boxes (E-box1, E-box2, and E-box3) were detected within the introns of *SMC2* (Fig. 2C). A chromatin immunoprecipitation (ChIP) assay was used to examine whether *MYCN* is able to bind to the identified E-boxes (Fig. 2D). When *MYCN* was overexpressed, the amount of *MYCN* that bound to E-box2

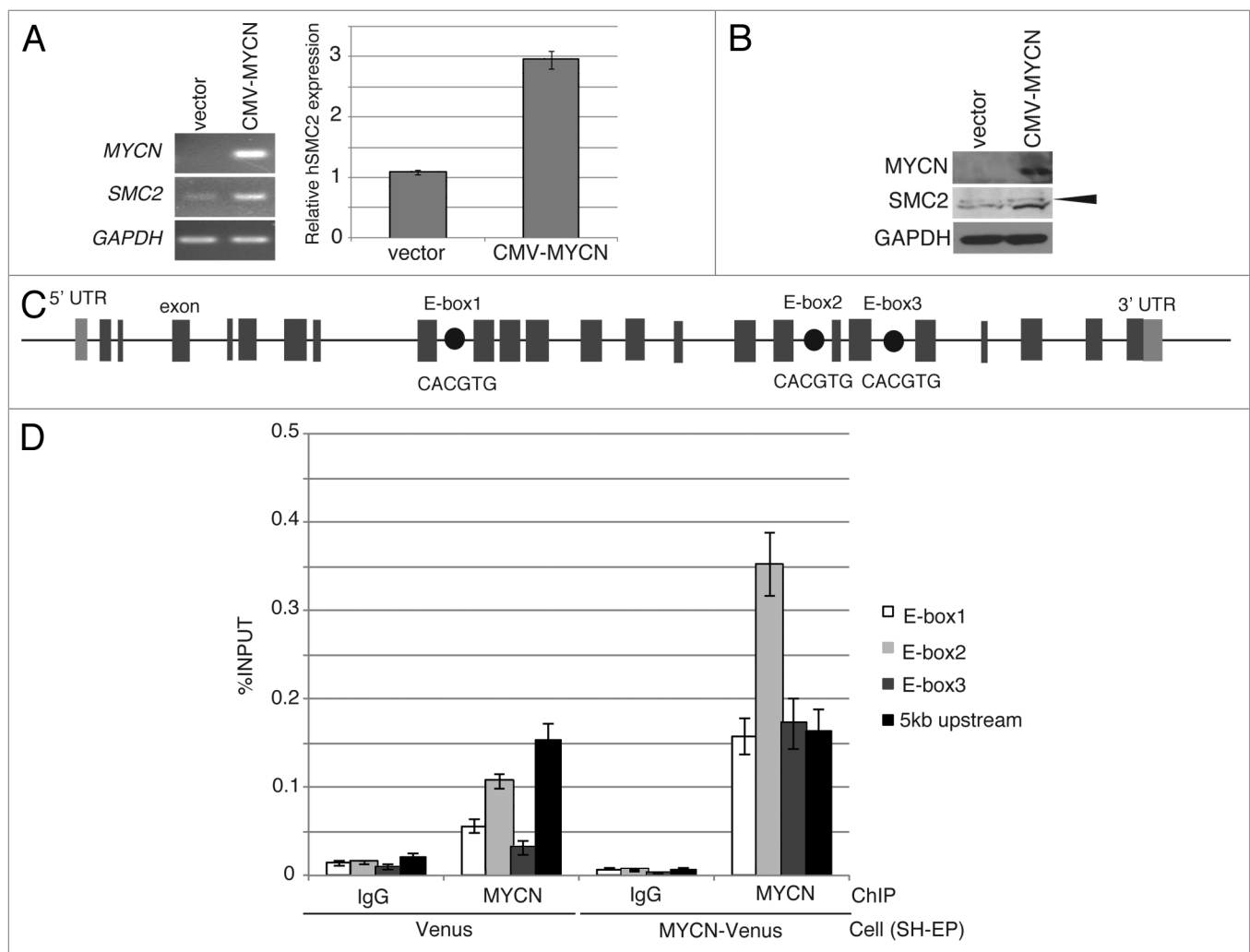


Figure 2. Overexpression of *MYCN* induces *SMC2* expression in human neuroblastoma cells. (A and B) A CMV-driven plasmid containing *MYCN* was introduced into the SH-EP *MYCN* single copy cell line. After live cell sorting, the levels of human *SMC2* mRNA and protein were measured by semi-quantitative (A, left) and quantitative (A, right) RT-PCR, as well as by immunoblotting (B). The arrowhead in (B) indicates a non-specific band. The expression levels of *SMC2* detected by RT-qPCR were normalized to those of *GAPDH*. (C) Schematic representation of the E-boxes identified in the human *SMC2* gene. The light gray boxes indicate the 5' and 3' UTRs; the dark gray boxes indicate the exons; and the black circles represent putative E-boxes (*MYCN*-binding sites). The sequences of the E-boxes are shown. (D) ChIP analysis of the E-boxes in the *SMC2* gene was performed using control IgG or an anti-*MYCN* antibody in SH-EP cells expressing Venus (control) or *MYCN*. The 5-kb sequence upstream of the *SMC2* gene was examined as a negative control. The data show the percentage of the target DNA precipitated with the control IgG or *MYCN* antibody and are represented as the mean \pm SE of at least $n = 3$ independent experiments.

increased (Fig. 2D). In the control cells, the amount of MYCN bound to E-box2 was also higher than the amount of IgG antibody bound to E-box2 (Fig. 2D); however, this difference is likely due to non-specific binding, because the amount of MYCN bound to the 5-kb upstream region also increased (Fig. 2D). These results indicate that MYCN regulates SMC2 expression by binding to its E-box2 motif.

Knockdown of *SMC2* induces DNA damage and apoptosis

A short hairpin RNA (shRNA) targeting *SMC2* inhibited proliferation of MYCN-overexpressing SH-EP cells but not of *MYCN* single copy control SH-EP cells (Fig. 3A). By contrast, the proliferation of MYCN-overexpressing SH-EP cells and control SH-EP cells infected with a non-target shRNA was similar (Fig. 3A), indicating that overexpression MYCN and a reduction in *SMC2* expression has a synergistic lethal response. The knockdown efficiency of each cell is shown in Figure 3B.

Next, a TUNEL assay was used to determine whether knockdown of *SMC2* and amplification of *MYCN* causes apoptosis. Very few FITC-positive cells were detected in non-infected or non-target shRNA-infected IMR32 cells, but almost all cells infected with *SMC2*-specific shRNA were FITC-positive (Fig. 3C). Most of the *SMC2*-knockdown IMR32 cells were TUNEL-positive at 6 d after virus infection. DNA damage induces apoptosis;⁴¹ therefore, the level of DNA damage in these cells was also examined. Histone H2A phosphorylation at a serine residue (γ -H2AX) is a sensitive marker of DSBs.⁴² The number of γ -H2AX-positive cells was markedly higher in *SMC2*-knockdown IMR32 and SK-N-BE(2) cells than in IMR32 and SK-N-BE(2) cells infected with a non-specific shRNA (Fig. 3D and E); however, the number of γ -H2AX-positive cells was not increased by knockdown of *SMC2* in the SK-N-AS and SH-EP cell lines. Most of the *SMC2*-knockdown IMR32 cells, and approximately 40% of the non-target shRNA-infected IMR32 cells, displayed γ -H2AX foci. The mechanism that induced DNA damage in the non-target lentivirus-infected *MYCN*-amplified cells is unknown. Despite this outcome, the results suggest that knockdown of *SMC2* induces additional DNA damage in *MYCN*-amplified cells.

The induction of ROS production or replication stress by MYC causes DNA damage.^{15,16}

Table 1. Mini-ontology of genes correlated with SMC2 expression from published human neuroblastoma expression array data sets (GSE16476, GSE3960, GSE13136) created using the R2 bioinformatic platform (<http://r2.amc.nl>)

GSE16476				
<i>SMC2</i> (204240_s_at)				
Group	InSet	Total	%	pval
All	560	8139	6.90%	1
DNA repair	63	208	30.30%	1.40E-40
TF	48	715	6.70%	0.86
apoptosis	38	595	6.40%	0.63
cell cycle	134	478	28.00%	1.40E-74
development	86	1421	6.10%	0.22
diff	39	585	6.70%	0.84
drugtarget	50	1056	4.70%	5.90E-03
kinase	39	615	6.30%	0.6
membrane	187	4123	4.50%	2.70E-09
sign transd	134	2469	5.40%	4.30E-03
transcription regulator Act	74	1093	6.80%	0.89
transcriptional repressor Act	13	174	7.50%	0.76
<i>SMC2</i> (213253_st)				
Group	InSet	Total	%	pval
All	271	8139	3.30%	1
DNA repair	45	208	21.60%	5.20E-49
TF	17	715	2.40%	0.16
apoptosis	17	595	2.90%	0.52
cell cycle	96	478	20.10%	1.20E-92
development	33	1421	2.30%	0.03
diff	18	585	3.10%	0.73
drugtarget	28	1056	2.70%	0.22
kinase	26	615	4.20%	0.21
membrane	65	4123	1.60%	3.50E-10
sign transd	52	2469	2.10%	7.00E-04
transcription regulator Act	28	1093	2.60%	0.16
transcriptional repressor Act	0	174	0.00%	0.01
GSE3960				
<i>SMC2</i> (37502_at)				
Group	InSet	Total	%	pval
All	392	5635	7.00%	1
DNA repair	43	155	27.70%	2.70E-24
TF	38	573	6.60%	0.76
apoptosis	31	476	6.50%	0.7
cell cycle	93	362	25.70%	1.30E-44
development	48	1153	4.20%	1.90E-04
diff	20	480	4.20%	0.02
drugtarget	42	945	4.40%	2.40E-03
kinase	32	478	6.70%	0.82

Table 1. Mini-ontology of genes correlated with SMC2 expression from published human neuroblastoma expression array data sets (GSE16476, GSE3960, GSE13136) created using the R2 bioinformatic platform (<http://r2.amc.nl>) (continued)

GSE3960				
membrane	121	2635	4.60%	1.80E-06
sign transd	101	1911	5.30%	4.10E-03
transcription regulator Act	74	848	8.70%	0.04
transcriptional repressor Act	17	136	12.50%	0.01
GSE13136				
SMC2(204240_s_at)				
DNA repair	16	205	7.80%	1.90E-16
TF	8	670	1.20%	0.81
apoptosis	5	572	0.90%	0.37
cell cycle	67	473	14.20%	6.70E-135
development	6	1337	0.40%	6.10E-03
diff	2	546	0.40%	0.05
drugtarget	8	994	0.80%	0.17
kinase	14	600	2.30%	0.03
membrane	7	3887	0.20%	7.30E-10
sign transd	19	2343	0.80%	0.04
transcription regulator Act	10	1042	1.00%	0.33
transcriptional repressor Act	0	172	0.00%	0.13
SMC2(213253_st)				
DNA repair	0	205	0.00%	0.78
TF	0	670	0.00%	0.61
apoptosis	0	572	0.00%	0.64
cell cycle	2	473	0.40%	2.30E-05
development	0	1337	0.00%	0.47
diff	0	546	0.00%	0.64
drugtarget	0	994	0.00%	0.53
kinase	0	600	0.00%	0.63
membrane	0	3887	0.00%	0.22
sign transd	1	2343	0.00%	0.93
transcription regulator Act	0	1042	0.00%	0.52
transcriptional repressor Act	0	172	0.00%	0.8

We hypothesized that overexpression of MYCN also induces DNA damage, most of which is repaired in the normal condition, thereby allowing *MYCN*-amplified cells to survive. However, once SMC2 expression is reduced, cells are unable to repair the DNA damage, resulting in subsequent cell death. If these hypotheses are correct, *SMC2*-knockdown cells would be expected to be sensitive to DNA damage even in *MYCN* single copy neuroblastoma cell lines. This hypothesis was tested by treating SH-EP cells, which contain a single copy of *MYCN*, with cisplatin and camptothecin to cause DNA damage. Cisplatin mainly causes intrastrand cross-linking,⁴³ whereas camptothecin, a topoisomerase I inhibitor, causes replication-dependent DSBs.⁴⁴ Treatment

of *SMC2*-knockdown SH-EP cells with cisplatin or camptothecin decreased cell viability (Fig. 3F, upper panels), and treatment of *SMC2*-knockdown MYCN-overexpressed SH-EP cells with cisplatin or camptothecin was more sensitive (Fig. 3F, lower panels). These results suggest that MYCN-induced DNA damage is required for the synergistic lethal response with *SMC2* knockdown.

SMC2 regulates the expression of DDR genes

We next investigated how SMC2 is involved in DNA damage repair. Table 1 shows mini-ontology data of 3 cohorts, which are available at the R2 microarray analysis and visualization platform (<http://r2.amc.nl>). The first cohort consisted of 88 neuroblastoma patients from the Academic Medical Center in Amsterdam,⁴⁵ the second cohort consisted of 101 neuroblastoma patients from the Children's Hospital of Philadelphia,⁴⁶ and the third cohort consisted of 30 neuroblastoma patients from the Leeds and Newcastle NHS Trusts.⁴⁷

DDR genes are involved in DNA repair. DDR gene expression increased in parallel with *SMC2* expression (Table 1), suggesting a relationship between *SMC2* expression and DDR gene expression. Some DDR genes, including *BRCA1*, *MRE11*, *NBS1*, *RAD50*, and *ATM*, are transcriptionally regulated by MYC.⁸⁻¹² To determine whether SMC2 is involved in controlling the transcription of DDR genes, qPCR analyses were used to measure the expression levels of some DDR genes regulated by MYC when *SMC2* was knocked down in single copy or in *MYCN*-amplified neuroblastoma cell lines. In IMR32 cells, knockdown of *SMC2* did not affect β -*ACTIN* transcription, but the levels of *BRCA1*, *MRE11*, *NBS1*, *RAD50*, and *ATM* mRNAs decreased (Fig. 4A, left panel). By contrast, knockdown of *SMC2* in SK-N-AS cells had a smaller effect on the expression levels of these genes (Fig. 4A, right panel). Similar results

were obtained when experiments were performed with MYCN-overexpressed SH-EP cells and control SH-EP cells (Fig. 4B). These results suggest that SMC2 regulates DDR gene expression in cooperation with MYCN.

MYCN interacts with SMC2 and SMC4

The possibility of an interaction between SMC2 and MYCN was investigated using a pull-down assay. The results indicated that SMC2, SMC4, and MYCN all interacted with each other (Fig. 4C). Choi and colleagues reported that MYCN associates with SMC4 and SMC2 in FLAG-tagged MYCN-expressing HeLa cells,⁴⁸ suggesting that this interaction occurs in multiple cell types.

The MYC binding site in the *NBS1* gene is the E-box within intron 1.¹¹ To test whether MYCN also binds to this motif, a ChIP analysis was performed using an anti-MYCN antibody. MYCN bound to the E-box motif in the *NBS1* gene (Fig. 4D, left panel). SMC2 bound to the same motif (Fig. 4D, right panel). These results suggest that SMC2 regulates *NBS1* transcription in cooperation with MYCN.

In addition, we found that the protein level of condensin subunit decreased when *SMC2* knockdown (Fig. 4E). This suggests that condensin complex becomes unstable when SMC2 is lost.

Genome-wide analysis of genes regulated by SMC2

To identify the genes regulated by SMC2, RNA-seq of *SMC2*-knockdown SH-EP cells constitutively expressing MYCN or Venus as a control was performed (SRA081723). A remarkable number of the genes that were induced or repressed in these cells were related to the DDR, DNA repair, or the cell cycle (Table 2; Table S1). The results indicated that knockdown of *SMC2* had a larger effect on *ATM* and *RAD50* transcription in SH-EP cells overexpressing MYCN than in the control cells, which agrees with the results of the RT-qPCR analyses shown in Figure 4A. These results suggest that SMC2 effects the expression of a number of genes involved in DNA repair, the DDR, and the cell cycle.

Analysis of the potential involvement of SMC2 in neurogenesis

High-risk neuroblastomas may have defects in neurogenesis genes.⁴⁹ During zebrafish development, *smc2* and *smc4* are expressed in some regions of the central nervous system,⁵⁰ and a mutation in the microcephalin gene deregulates condensin II and causes autosomal recessive primary microcephaly.⁵¹ Therefore, we re-analyzed mouse expression array data published in ArrayExpress (E-GEOD-11356, <http://www.ebi.ac.uk/microarray-as/ael/>). *Mycn* was highly expressed in E8.5 (neural tube closure) samples and gradually decreased in E13.5 (dorsal root ganglion) and P90 (adrenal medulla) samples. The expression pattern of *Smc2* was similar to that of *Mycn* (Fig. S1). These data suggest that, along with MYCN, SMC2 (or the condensin complex) may have a role in sympathetic neurogenesis.

Clinical data

We hypothesized that patients bearing *MYCN*-amplified tumors would benefit from low SMC2 expression. Therefore, we investigated whether *SMC2* expression correlated with patient prognosis in a previous cohort used by Wang et al.⁴⁶ In *MYCN*-amplified patients, low levels of *SMC2* were associated with good prognosis (overall survival, $P = 0.051$; event-free survival, $P = 0.053$) (Fig. 5A). These results indicate that low *SMC2* expression in *MYCN*-amplified patients tends to correlate with good prognosis.

The expression levels of other condensin I and II subunits were higher in precancerous and tumor lesions

Table 2. List of induced or repressed GO categories belonging to DDR, DNA repair, and cell cycle-related classes in *SMC2*-knockdown Venus- or MYCN-expressing SH-EP cells. Non-target shRNA-infected cells were used as a control

Gene ontology classes enriched in <i>SMC2</i> -knockdown Venus-expressing SH-EP cells			
GO term	Total No. genes in set	No. genes regulated	P value
cell cycle	828	225	2.55E-12
cell cycle process	647	185	5.77E-12
cell cycle phase	548	158	2.52E-10
mitotic cell cycle	470	139	5.97E-10
DNA metabolic process	594	157	1.58E-07
regulation of cell cycle	526	139	2.00E-06
M phase	344	97	1.95E-05
chromosome	471	124	1.72E-05
interphase of mitotic cell cycle	257	76	7.92E-05
M phase of mitotic cell cycle	246	73	1.19E-04
interphase	261	76	1.37E-04
G1/S transition of mitotic cell cycle	126	45	1.21E-04
mitosis	239	71	1.44E-04
chromosome, centromeric region	124	44	1.72E-04
chromosome segregation	98	37	2.82E-04
cell division	295	82	3.30E-04
condensed chromosome, centromeric region	69	29	3.80E-04
chromosome organization	518	125	0.001
mitotic prometaphase	73	29	0.001
regulation of cell cycle process	292	78	0.003
condensed chromosome	124	41	0.003
condensed chromosome kinetochore	64	25	0.008
DNA replication	147	45	0.008
response to DNA damage stimulus	427	103	0.009
DNA conformation change	159	47	0.013
chromatin	206	56	0.028
negative regulation of cell cycle	194	53	0.037
cell cycle checkpoint	180	50	0.037
DNA repair	287	72	0.041
kinetochore	75	26	0.047
chromatin remodeling	67	24	0.049

Table 2. List of induced or repressed GO categories belonging to DDR, DNA repair, and cell cycle-related classes in *SMC2*-knockdown Venus- or *MYCN*-expressing SH-EP cells. Non-target shRNA-infected cells were used as a control (continued)

Gene ontology classes enriched in <i>SMC2</i> -knockdown <i>MYCN</i> -expressing SH-EP cells			
GO term	Total No. genes in set	No. genes regulated	<i>P</i> value
gene expression	1680	581	3.86E-15
response to DNA damage stimulus	427	179	1.29E-10
DNA metabolic process	594	223	1.36E-10
cell cycle process	647	244	4.60E-09
mitotic cell cycle	470	188	4.64E-09
cell cycle	828	299	5.90E-09
chromatin modification	328	139	2.72E-08
DNA repair	287	124	7.03E-08
covalent chromatin modification	194	90	3.67E-07
histone modification	192	89	4.78E-07
cell cycle phase	548	204	8.24E-07
regulation of gene expression	2625	796	1.02E-06
chromosome organization	518	194	1.18E-06
chromatin organization	396	154	3.28E-06
transcription factor binding	284	116	1.18E-05
regulation of cell cycle	526	191	2.23E-05
cell division	295	118	3.28E-05
mitosis	239	98	1.05E-04
chromosome	471	171	1.05E-04
M phase of mitotic cell cycle	246	100	1.25E-04
chromosome, centromeric region	124	58	2.26E-04
regulation of transcription, DNA-dependent	2324	692	3.00E-04
transcription cofactor activity	345	130	3.10E-04
protein binding transcription factor activity	352	132	3.42E-04
transcription factor binding transcription factor activity	349	131	3.52E-04
condensed chromosome, centromeric region	69	37	4.79E-04
interphase of mitotic cell cycle	257	101	6.15E-04
interphase	261	102	7.27E-04
M phase	344	127	0.001
regulation of gene expression, epigenetic	96	46	0.001
chromatin remodeling	67	35	0.002
chromosomal part	389	140	0.002

from *MYCN* Tg mice than in wt mouse ganglion samples; however, the difference was less pronounced than that observed for *Smc2* (Fig. S2). Table S2 shows mini-ontology data of three cohorts available at the R2 bio-informatic platform (<http://r2.amc.nl>). The expression levels of most of the condensin I and II subunits correlated with DDR gene expression. We also examined the expression levels of the condensin subunits in the Wang cohort.⁴⁶ Expression of the condensin I-specific subunits was related to the level of *MYCN* amplification or expression, whereas the expression of condensin II-specific subunits was not (Fig. 5B). Figure S3 shows the relationship among *MYCN* expression, condensin subunit expression, and prognosis of 101 neuroblastoma patients included in the Wang cohort.⁴⁶ We separated the samples into 2 groups, namely *MYCN* high expression and *MYCN* low expression. If patients bearing *MYCN*-high tumors benefit from low condensin subunit expression, only the subunit-high group of *MYCN*-high patients would show poor prognosis. That means only *MYCN*-high group would show the significant difference ($P < 0.05$). Figure S3 shows that patients expressing high levels of *MYCN* and condensin I subunit (CAP-D2) or *SMC4* had poor prognosis, although prognosis of those expressing condensin I subunit (CAP-H) was not always related to *MYCN* expression. However, prognosis of patients expressing condensin II subunit was not related to *MYCN* expression. These results suggest that *SMC2* may function as a condensin complex (probably as condensin I), rather than alone, in this phenotype.

Discussion

This study demonstrates that (1) *SMC2* is regulated by *MYCN*; (2) *SMC2*, in cooperation with *MYCN*, regulates DDR genes; and (3) downregulation of *SMC2* and concomitant *MYCN* amplification induces DNA damage and has a synergistic lethal effect, resulting in apoptosis of human neuroblastoma cells. This study also demonstrates that patients bearing *MYCN*-amplified tumors tend to benefit from low *SMC2* expression. A model summarizing these findings is shown in Figure 6. In *MYCN*-amplified cells, *MYCN* induces DNA damage, most likely via the production of ROS and replicative stress. On the other hand, since *SMC2* is overexpressed in these cells, the DDR may also be highly activated. As a consequence, cells are viable, but some mutations would still remain (Fig. 6A, left). In this situation, knockdown of *SMC2* would impair the DDR, resulting in cell death (Fig. 6A, right). By contrast, in *MYCN* single copy cells, the extent of DNA damage is lower, and knockdown of *SMC2* does not affect cell viability (Fig. 6B).

Several reports have suggested that the condensin complex is required for the recruitment of DNA repair proteins to damage sites.^{2,52,53} In this study, we found that *SMC2* interacts with *MYCN* and is involved in

Table 2. List of induced or repressed GO categories belonging to DDR, DNA repair, and cell cycle-related classes in *SMC2*-knockdown Venus- or *MYCN*-expressing SH-EP cells. Non-target shRNA-infected cells were used as a control (continued)

Gene ontology classes enriched in <i>SMC2</i> -knockdown <i>MYCN</i> -expressing SH-EP cells			
negative regulation of gene expression	580	197	0.002
mitotic prometaphase	73	37	0.002
DNA-dependent transcription, initiation	76	38	0.002
positive regulation of transcription, DNA-dependent	664	220	0.003
condensed chromosome kinetochore	64	33	0.004
cell cycle checkpoint	180	72	0.008
posttranscriptional regulation of gene expression	243	92	0.008
transcription, DNA-dependent	794	254	0.01
condensed chromosome	124	53	0.011
regulation of transcription from RNA polymerase II promoter	792	253	0.011
positive regulation of gene expression	712	230	0.011
chromosome segregation	98	44	0.012
transcription initiation from RNA polymerase II promoter	51	27	0.012
regulation of cell cycle process	292	106	0.013
transcription coactivator activity	197	76	0.016
regulation of cell cycle arrest	188	73	0.017
spindle	160	64	0.018
DNA recombination	130	54	0.02
kinetochore	75	35	0.025
microtubule organizing center	326	114	0.035
negative regulation of transcription, DNA-dependent	521	171	0.039
protein serine/threonine kinase activity	364	125	0.039
DNA damage response, signal transduction by p53 class mediator	71	33	0.04
G ₂ /M transition of mitotic cell cycle	101	43	0.049

transcriptional regulation of DDR genes, and that *SMC2* expression is regulated by *MYCN* as well as by Wnt⁵⁴ (Fig. 6C). There are several advantages of using *SMC2* as a molecular target for the treatment of *MYCN*-amplified neuroblastoma. First, knockdown of *SMC2* has similar effects to knockdown of several DDR genes. Second, if *MYC* functions similarly to *MYCN*, inhibition of *SMC2* would be expected to have growth-inhibitory activity

in *MYC*-overexpressed/amplified cancers. If so, *SMC2* knockdown is a powerful tool for both *MYCN*- and *MYC*-overexpressed/amplified cancers.

There are still some unanswered questions. First, other than *MYCN*, which other transcription factors interact with *SMC2* or the condensin complex? CAP-G associates with bHLH transcription factors in erythroid cells;⁵ therefore, *SMC2* (or the condensin complex) may cooperate with various transcription factors in different tissues or developmental stages. The second question relates to the mechanism by which *SMC2* is involved in transcriptional regulation. *SMC2* associates with *MYCN*, but its specific role in the *MYCN* complex remains unknown. *SMC2* may act as a co-factor or alter the chromosomal conformation. Third, what is the functional difference between *MYC* and *MYCN*? *MYCN*-amplified neuroblastoma cells express low levels of *MYC*, while *MYCN* single copy neuroblastoma cells express higher levels.²⁴ As described above, knockdown of *SMC2* had a synergistic lethal effect with amplification or overexpression of *MYCN*, but this effect was not seen in *MYCN* single copy cells. This result implies that knockdown of *SMC2* is synergistic lethal with *MYCN* but not with *MYC*. It might also suggest that the gene set that shows a synergistic lethal effect with *MYCN* is different from that associated with *MYC* amplification or overexpression. CDK2,²⁶ Aurora A,²⁷ and CHK1²² kinases show specific synergistic lethal responses with *MYCN*, but not with *MYC* in *MYCN* single copy cells. However, another report demonstrated that *MYC* and *MYCN* are functionally redundant to some extent,⁵⁵ and the gene(s) that are synthetic lethal with *MYC* overexpression in human foreskin fibroblasts are also synthetic lethal with *MYCN*, but not with *MYC* in *MYCN* single copy cells.^{24,56} Further studies are required to elucidate the relationship between *MYC* and *MYCN*.

Materials and Methods

Mice

*MYCN*Tg mice³⁸ were maintained in the animal facility at Nagoya University Graduate School of Medicine where they were housed in a controlled environment and provided with standard nourishment and water. Normal ganglia and precancerous and tumor tissues from wt, hemizygous, and homozygous *MYCN* Tg mice were dissected and minced, and then total RNA was extracted. This study was approved by the Animal Care and Use Committee of Nagoya University Graduate School of Medicine, Nagoya, Japan.

Gene expression profiling

Total RNA was isolated using ISOGEN reagent (Nippon Gene), according to the manufacturer's instructions. Samples were analyzed with a GeneChip Mouse Genome 430 2.0 array (Affymetrix). Preparation of target cDNA from total RNA, hybridization to the microarray, washing, staining with an

antibody amplification procedure, and scanning were all performed according to the manufacturer's instructions. The expression value (Signal) of each probe set was calculated using GeneChip Operating Software (GCOS) version 1.3 (Affymetrix). The data described in this manuscript have been deposited in the Gene Expression Omnibus database of NCBI (<http://www.ncbi.nlm.nih.gov/geo>) under the accession number GSE43419.

Cell lines, virus infection, and transfection

IMR32 cells were obtained from JCRB (JCRB9050); 293T (RCB2202) cells were obtained from the RIKEN Cell Bank; SH-SY5Y, SK-N-AS, and SK-N-BE(2) cells were purchased from ATCC (CRL-2266, CRL-2137, and CRL-2271); SH-EP cells were a gift from Dr Schwab (Division of Tumor Genetics,

German Cancer Research Center), and NB39 cells were a gift from Dr Chiba (Fukushima Medical University).

IMR32 cells were grown in minimum essential medium (Sigma) supplemented with 10% fetal bovine serum (HyClone, Thermo Scientific) and 1% non-essential amino acids (GIBCO-Life Technologies). SK-N-AS cells were grown in Dulbecco modified Eagle medium (MP Biomedicals, LLC) supplemented with 10% fetal bovine serum and 1% non-essential amino acids. SK-N-BE(2) and SH-SY5Y cells were grown in a 1:1 ratio of minimum essential medium and Ham-F12 (GIBCO-Life Technologies) supplemented with 10% fetal bovine serum (HyClone, Thermo scientific), 1% sodium pyruvate (Sigma), 1% GlutaMAX (GIBCO-Life Technologies), and 1% non-essential

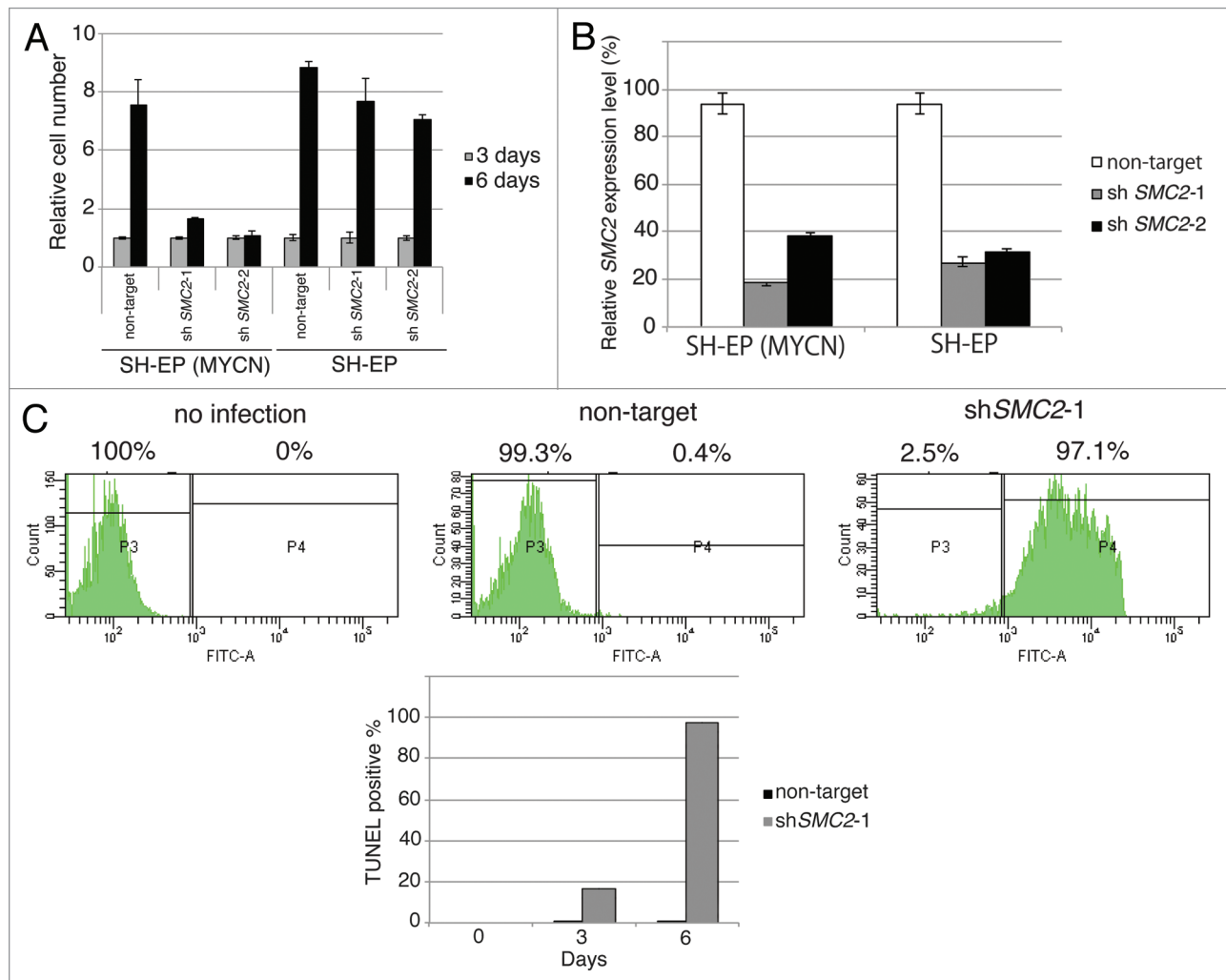


Figure 3A–C (See pages 1124 and 1125 for D–F). Knockdown of *SMC2* induces DNA damage and apoptosis. **(A)** Growth of MYCN-overexpressed SH-EP cells and control SH-EP cells infected with non-target shRNA or *SMC2*-specific shRNAs. Counting started 3 d after infection. On each day, 3 plates were counted and averaged. Data are shown as a ratio of the number of cells at 3 d after transfection and are represented as the mean \pm SD of $n = 3$ independent repeats. **(B)** *SMC2* knockdown efficiency of **(A)**. **(C)** TUNEL staining of apoptotic IMR32 cells at 6 d after infection (upper panel) and quantification of apoptotic IMR32 cells at the indicated time-points (lower panel). On each day, 3 plates were counted and averaged. **(D)** Immunofluorescence of γ -H2AX and DAPI staining of IMR32 (*MYCN*-amplified), SK-N-BE(2) (*MYCN*-amplified), SK-N-AS (*MYCN*-single copy), and SH-EP (*MYCN*-single copy) cells infected with non-target or *SMC2*-specific shRNA. Images were captured 3 d after infection. **(E)** Quantification of the γ -H2AX-positive cells shown in **(D)**. Data are represented as the mean \pm SD of $n = 3$ independent repeats. Their homoscedasticities were checked by *f* test. Statistical significance was evaluated with a 2-tailed, unpaired *t* test. **(F)** The percentage viability of SH-EP or MYCN overexpressed SH-EP cells infected with non-target or *SMC2*-specific shRNA and treated with cisplatin (left) or camptothecin (right). Data are represented as the mean \pm SE of $n = 3$ independent experiments. Their homoscedasticities were checked by *f* test. Statistical significance was evaluated with a 2-tailed, unpaired *t* test.

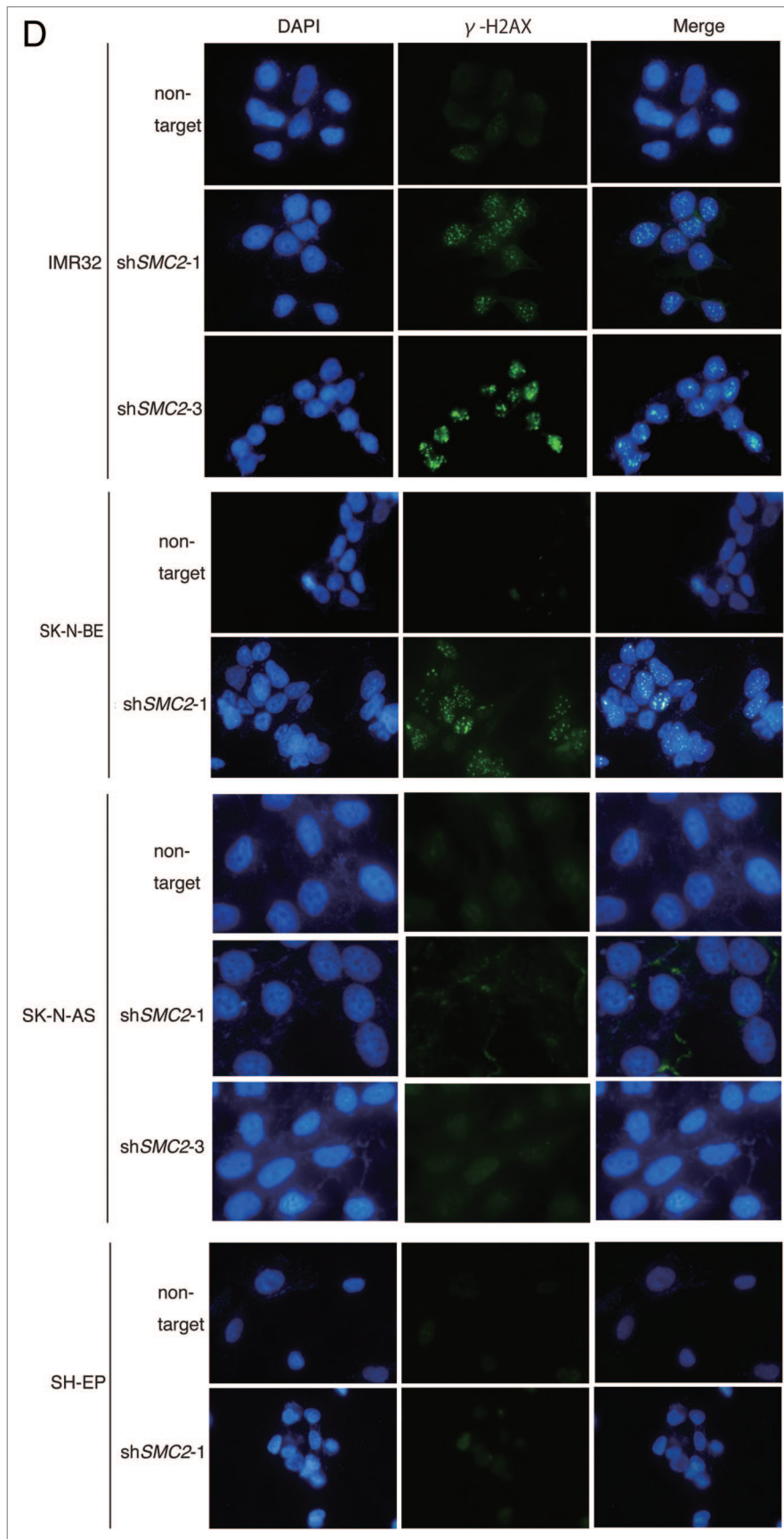


Figure 3D. For legend, see page 1123.

amino acids. 293T cells were grown in Dulbecco modified Eagle medium supplemented with 10% fetal bovine serum. SH-EP cells were grown in RPMI1640 (Sigma) supplemented with 10% fetal bovine serum.

Replication-defective, self-inactivating lentiviral vectors were used.^{57,58} HEK293T cells were co-transfected with shRNA plasmids in addition to psPAX2 (Addgene) and pMD2.G (Addgene) or cDNA expression plasmids. Neuroblastoma cell lines were infected in the presence of 15 μ g/ml polybrene (Sigma). 293T cells were transfected with various plasmids using FuGENE HD reagent (Promega), according to the manufacturer's instructions.

Plasmids

Constructs were generated by PCR using specific primers and a gateway cassette containing a full-length clone of human MYCN. This fragment was initially cloned into pDONR221 (Invitrogen) and then into the CSII-CMV-RfA-IRES-Venus plasmid. The successful introduction of this fragment into each construct was confirmed by DNA sequencing. The CSII-CMV-RfA-IRES-Venus plasmid and the CSII-CMV-Venus control plasmid were kindly provided by H Miyoshi (RIKEN). Commercially available non-targeting (Sigma) and SMC2-specific shRNA vectors (TRCN0000062540, TRCN0000062542, TRCN0000062538; Thermo Scientific Open Biosystems) were used. The shRNA sequences are listed in Table S3.

For pull-down and ChIP assays, the following Halo-tag Flexi ORF clones (Promega) were used: Halo-control (G6591), Halo-SMC2 (pFN21AE9255), Halo-SMC4 (pFN21AB7320), and Halo-MYCN (pFN21AB8396). A list of the plasmids used in the study is provided in Table S4. Further details are available upon request.

DNA damaging agents

Cells were treated with cisplatin (NIPPON-KAYAKU) or camptothecin (Sigma). Treatments were performed at 37 $^{\circ}$ C for overnight and at 14 μ M (for SH-EP cells) or 7 μ M (for MYCN-overexpressed SH-EP cells) cisplatin and 0.05 μ g/ml camptothecin.

Primers

The sequences of the primers used in the study are listed in Table S5.

Isolation of RNA, RT-PCR, and qPCR

Total RNA was isolated from cells or tissues using ISOGEN II reagent (Nippongene, Japan). For RT-PCR and RT-qPCR analyses, total RNA (1 μ g) was incubated with DNase I (Invitrogen) to eliminate contaminating genomic DNA, and then reverse transcribed with oligo(dT) and random hexamer primers and the ThermoScript RT-PCR system (Invitrogen). Quantitative PCR analyses were performed using an Mx3000p or Mx3005p instrument (Agilent Technologies) and the KAPA SYBR Fast qPCR kit (KAPA Biosystems). The expression levels of mouse *Smc2* and *Gapdh* (control), and human *SMC2*, *MYCN*, *GAPDH* (control), *BRCA1*, *MRE11*, *NBS1*, *RAD50*, *ATM*, and β -ACTIN were determined using the $\Delta\Delta$ CT method.

TUNEL assay

The TUNEL assay was performed using the APO-DIRECT kit (556381, BD Pharmingen). The manufacturer's protocol for cell fixation and staining was followed and then the APO-DIRECT samples were analyzed using a FACSCanto flow cytometer (BD Pharmingen) and Diva software.

Antibodies

The following antibodies were used: anti-MYCN monoclonal antibodies (OP13, Calbiochem and NB200-109, Novus Biologicals); anti-MYCN monoclonal antibody (B8.4.B) (sc-53993, Santa Cruz); anti-SMC2 rabbit polyclonal antibodies (GTx10411, GeneTex; and ab10412, Abcam); anti- β -ACTIN monoclonal antibody (AC-15) (A5441, Sigma); anti-SMC4 rabbit polyclonal antibody (ab17958, Abcam); anti-CAP-D2 rabbit polyclonal antibody (A300-601A, Bethyl Laboratories); and anti-phospho-histone H2A.X (Ser139) mouse monoclonal antibody (JBW301, Millipore).

Immunofluorescence

For immunofluorescence, cells were grown on glass coverslips in 4- or 8-well plates. The coverslips were washed twice with phosphate-buffered saline (PBS) and then fixed with 4% paraformaldehyde for 1 h at room temperature. Fixed cells were washed with PBS a further 3 times and permeabilized with PBS containing 1% Triton X-100 for 30 min at room temperature. The cells were incubated with an anti- γ -H2AX antibody (1:1000 dilution) for 1 h at room temperature and then with Alexa Fluor 488-conjugated anti-mouse IgG (Molecular Probes) (1:1000 dilution) for 30 min at room temperature. After incubation for 5 min with 0.1 μ g/ml 4'-diamidino-2-phenylindole, cells were mounted in FluorSave Reagent (Millipore). All images were subsequently processed using MetaMorph and Adobe Photoshop.

Protein preparation and immunoblotting

Cells were washed with ice-cold PBS and then lysed with RIPA buffer (50 mM Tris-HCl [pH 8.0], 150 mM NaCl, 1% NP-40, 1% deoxycholic acid sodium salt monohydrate, 0.1% sodium dodecyl sulfate, and 1% protease inhibitor cocktail). Cell lysates were centrifuged at 4 $^{\circ}$ C for 10 min at 22,140 g and then analyzed by 10% PAGE. Proteins were transferred to PVDF membranes, which were then blocked for 1 h with PBS containing 5% non-fat dried milk and 0.05% Tween-20. The membranes were washed, probed with primary antibodies, and then exposed to horseradish peroxidase-conjugated secondary antibodies. Blots

were visualized using ECL reagent (GE Healthcare) and autoradiography film.

Pull-down assay

The HaloTag Mammalian Pull-Down System (Promega) was used according to the manufacturer's instructions. CMV-driven MYCN with CMV-driven Halo-control, Halo-SMC2, or Halo-SMC4, and Halo-MYCN proteins were expressed in 293T cells. Cells were harvested 64 h after transfection, according to the manufacturer's protocol. Briefly, HaloTag fusion proteins, along with their interacting proteins, were captured using the HaloLink resin and washed gently. Interacting proteins were eluted from the resin with SDS elution buffer and subjected to SDS-PAGE followed by electroblotting.

ChIP

Sub-confluent SH-EP cells expressing Venus or MYCN and IMR32 were cultured in 10-cm dishes and treated with 1% (v/v) formaldehyde for 10 min at room temperature. Cross-linking was stopped by adding glycine to a final concentration of 125 mM.

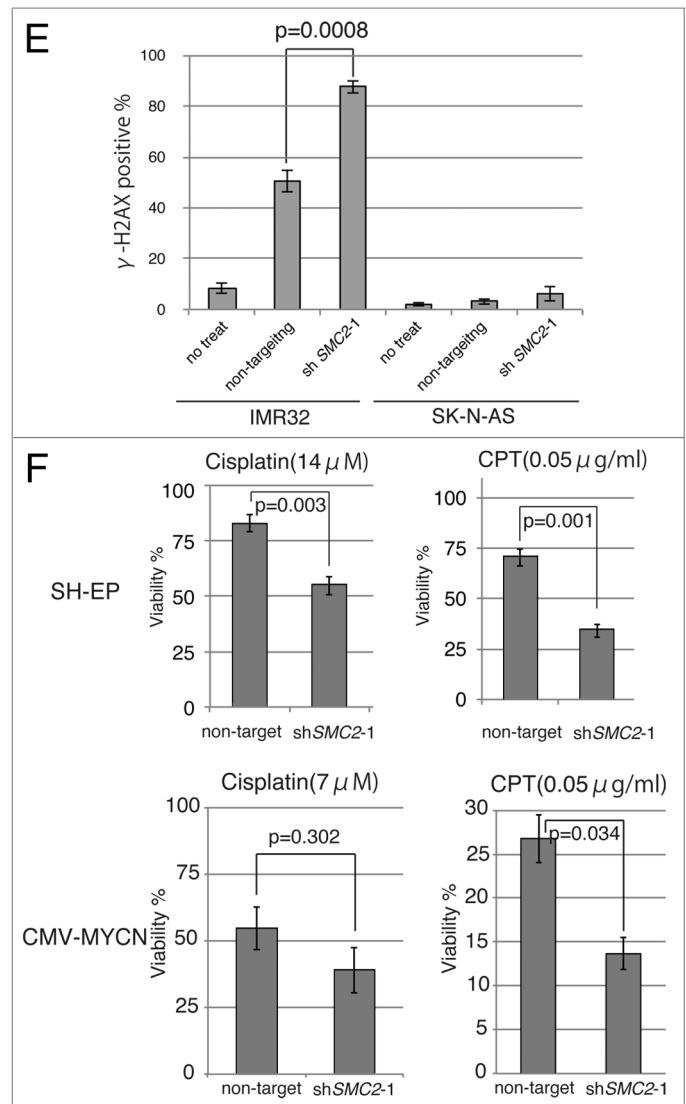


Figure 3E and F. For legend, see page 1123.

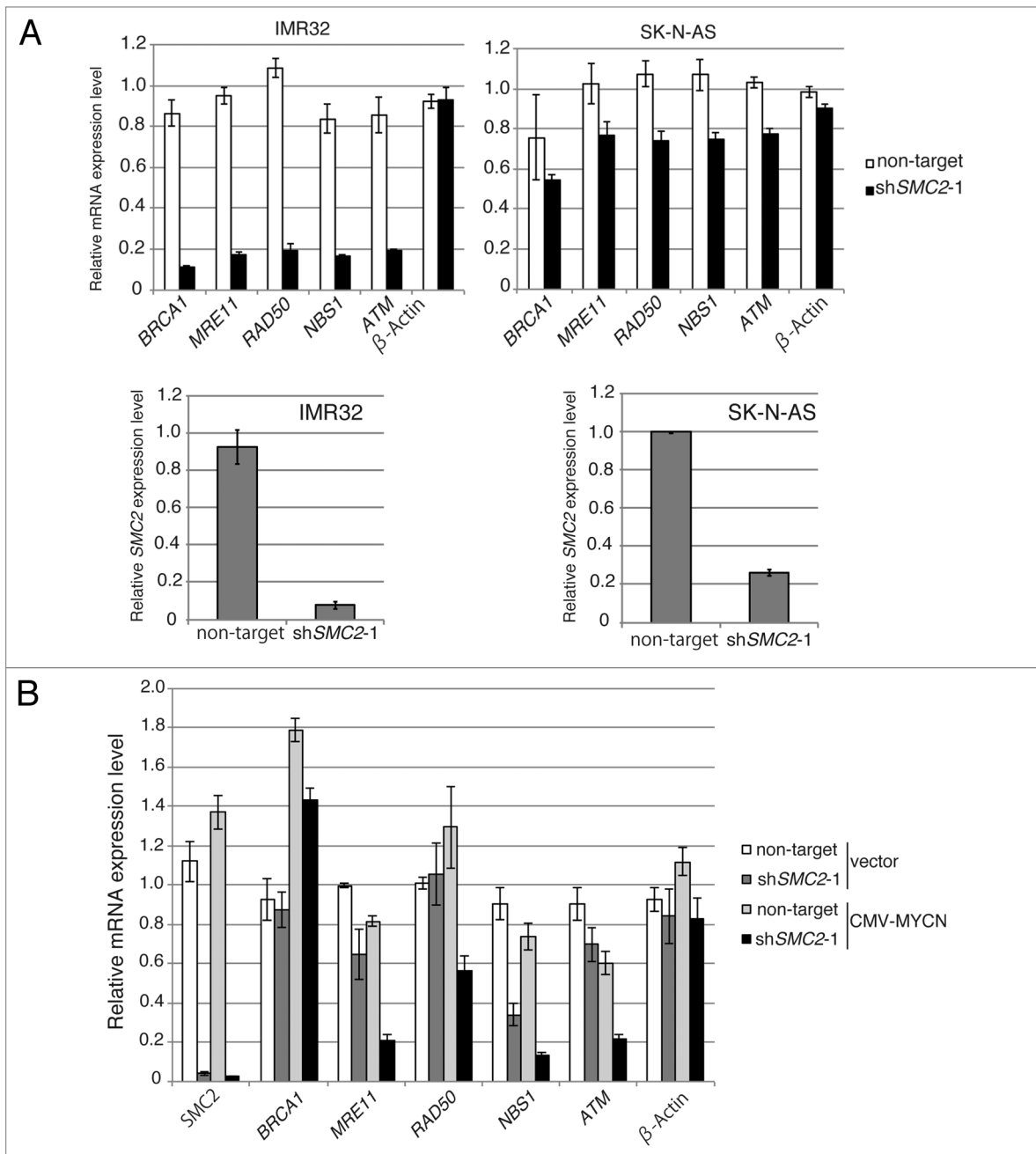


Figure 4A and B (See opposite page for C–E). SMC2 interacts with MYCN and transcriptionally regulates DDR genes. **(A)** RT-qPCR analysis of the relative expression levels of DDR genes in IMR32 cells (*MYCN*-amplified, top-left panel) and SK-N-AS cells (*MYCN* single copy, top-right panel) infected with non-targeting or *SMC2*-specific shRNA. Expression levels in *SMC2*-specific shRNA-infected cells were normalized to those in the control cells. Bottom panels are shown *SMC2* knockdown efficiency in each cells. **(B)** RT-qPCR analysis of the relative expression levels of DDR genes in MYCN-overexpressed SH-EP cells and control SH-EP cells as similar in **(A)**. **(C)** Pull-down assay showing that MYCN interacts with SMC2 and SMC4. CMV-driven MYCN, along with CMV-driven Halo-control, Halo-SMC2 or Halo-SMC4 and Halo-MYCN proteins were expressed in 293T cells. A pull-down assay was performed using a Halo-tag. The proteins were detected with the indicated antibodies. WCE (TMR), TMR Direct ligand stained Halo-tag proteins in whole-cell extract. **(D)** SMC2 and MYCN bind to the E-box motif in the *NBS1* gene. The left panel shows the results of a ChIP assay of the E-box in the *NBS1* gene performed using an anti-MYCN antibody in cells expressing Venus (control) or MYCN. The right panel shows the results of a ChIP assay of the E-box in the *NBS1* gene performed using an anti-SMC2 antibody in *MYCN*-amplified IMR32 cells. A region situated 14.5 kb upstream of the E-box was used as a negative control. Data show the percentages of the target DNA precipitated with the antibodies and are represented as the mean \pm SE of at least $n = 3$ independent qPCR experiments. **(E)** The protein level of SMC4 and CAP-D2 when SMC2 is knockdown in MYCN-expressing SH-EP (*MYCN* single copy) cells and control Venus-expressing SH-EP cells. β -ACTIN is used as loading control.

The cells were washed with cold PBS and then harvested. The cells were pelleted, frozen at -70°C , and then lysed by mechanical disruption. The Halo-ChIP system (Promega) was then used according to the manufacturer's instructions, except that an anti-MYCN antibody and Dynabeads-protein G (Dyna) were used. DNA was purified twice using phenol-CIAA. The purified DNA was PCR-amplified using primers spanning the MYCN-binding site in the *SMC2* and *NBS1* genes. Cells immunoprecipitated with control IgGs were used as a negative control.

RNA-seq analysis

Cells were harvested 72 h after infection with non-target or *SMC2*-specific lentiviruses. Total RNA was prepared from the cells using the RNeasy mini kit (Qiagen), according to the manufacturer's instruction. The TruSeq RNA Sample Preparation

Kit v2 (Illumina, Inc) was used to prepare RNA-Seq libraries following the manufacturer's instructions. Libraries were sequenced with the Illumina HiSeq 2500 sequencer for 50-bp single read. The data described in this manuscript have been deposited in the Sequence Read Archive database of NCBI (<http://www.ncbi.nlm.nih.gov/sra>) under the accession number SRA081723.

Analysis of human neuroblastoma tumor profiles

Three clinical neuroblastoma gene expression data sets were used for the analysis. As described by Molenaar et al.⁴⁹ (accession number: GSE16476, www.ncbi.nlm.nih.gov/geo), Wang et al.⁵⁹ (accession number: GSE3960, www.ncbi.nlm.nih.gov/geo), and Lastowska et al.⁴⁷ (accession number: GSE13136, www.ncbi.nlm.nih.gov/geo), the basis of these data sets differs markedly, both with

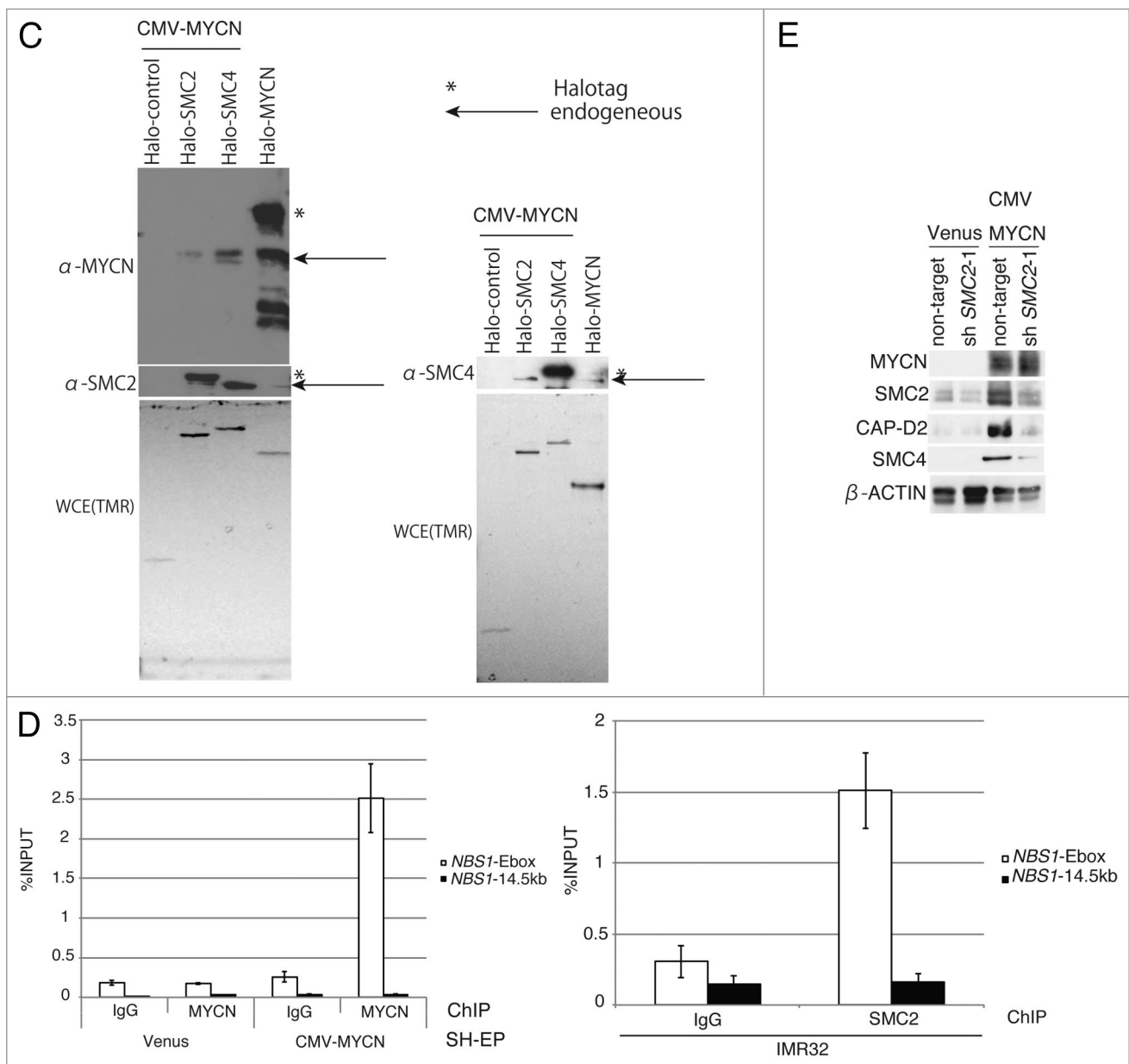


Figure 4C-E. For legend, see page 1126.

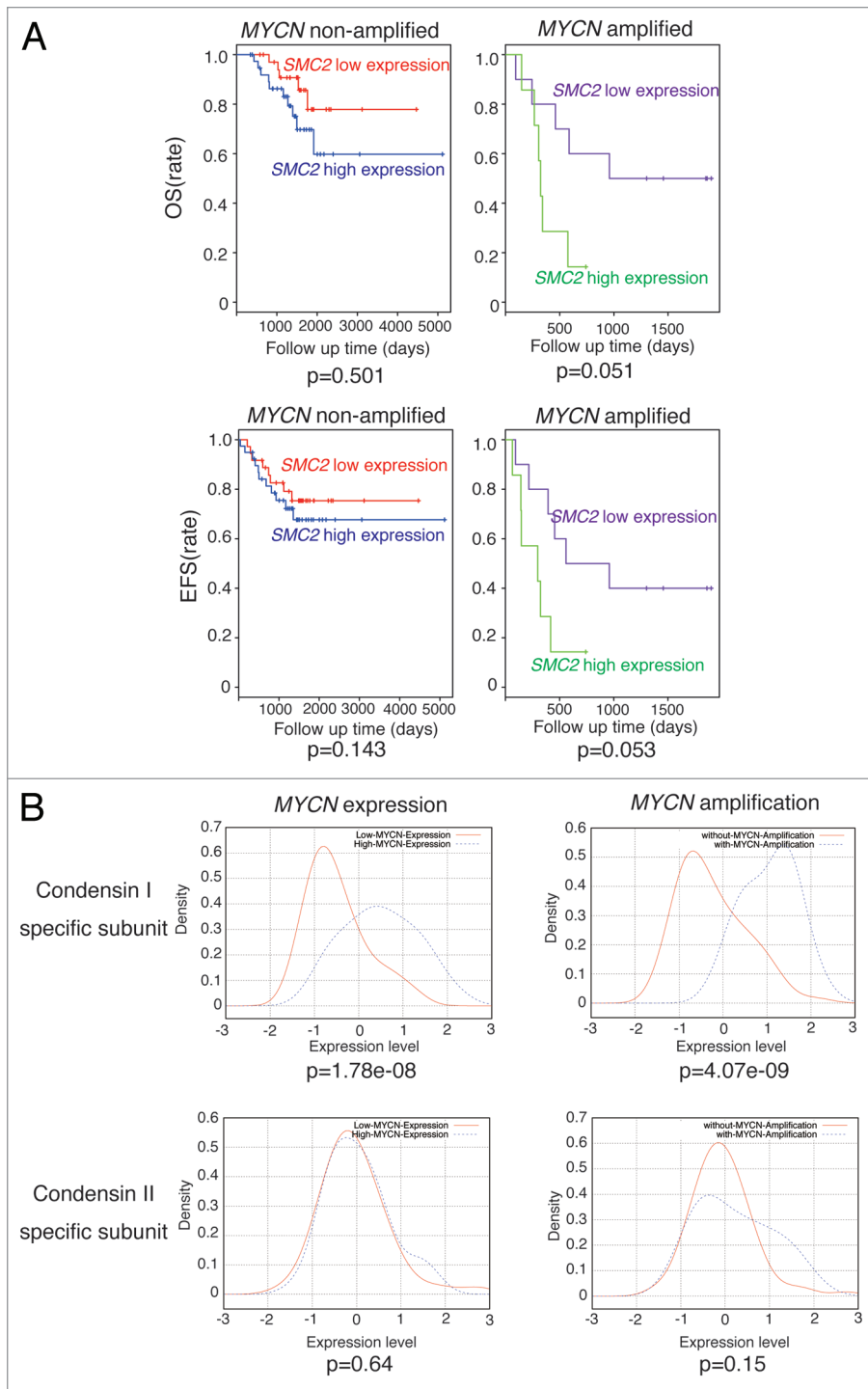


Figure 5. Clinical data showing the relationship between *SMC2* expression and patient prognosis in the Wang cohort.⁴⁸ (A) The effects of *SMC2* expression on the overall survival (OS) and event-free survival (EFS) rates of patients bearing *MYCN*-amplified and non-amplified tumors. Within each of the 2 tumor subsets considered, those with expression levels of *SMC2* greater than the median (blue or green line) were compared with the remainder of the tumors in the subset (red or purple line) using a Kaplan–Meier analysis. (B) Expression levels of condensin I- and condensin II-specific subunits and their relationship to *MYCN* amplification or expression. The data were obtained from a published data set (GSE3960). The red line indicates low *MYCN* expression or no *MYCN* amplification, and the blue line indicates high *MYCN* expression or *MYCN* amplification.

respect to the selection of patient cohorts and to the microarray technologies used. The Molenaar data included 88 patients and microarrays were performed using the Affymetrix Human Genome U133 Plus 2.0 array. The Wang data included 101 cases, and microarrays were performed using the Affymetrix HgU95Av2 array. The Lastowska data included 30 neuroblastomas and microarrays were performed using the Affymetrix Human Genome U133 Plus 2.0 array. For the Molenaar, Wang, and Lastowska studies, the normalized microarray data deposited in the Gene Expression Omnibus database were used. For the Wang data, quality filtration was applied as described previously.⁴⁶

In Figure 5A, we analyzed the gene expression and survival data in Wang cohort study.⁴⁸ We divided the entire sample into four groups: (red) those with non-*MYCN* amplification and the *SMC2* expression levels lower than the median value; (blue) those with non-*MYCN* amplification and the *SMC2* expression levels higher than the median value; (green) those with *MYCN* amplification and the *SMC2* expression levels higher than the median value; (purple) those with *MYCN* amplification and the *SMC2* expression levels lower than the median value. Then, the significance of the difference in survival between red vs. blue and green vs. purple are examined by using Kaplan–Meier plots and Log-rank test. The top 2 panels are plots with overall survival, whereas the bottom 2 panels are with event-free survival. In Figure 5B, we divided the entire sample of published data set (GSE3960) into those with higher and lower *MYCN* expressions than the median value. The plotted are the density estimates (density estimate is considered as a smoothed histogram which can be computed by using kernel density estimation algorithm *kde* in R) of condensin I- and condensin II-specific subunits. The given *P* values dictate the significance of the difference between 2 expression densities (by using *U* test).

Disclosure of Potential Conflicts of Interest

No potential conflicts of interest were disclosed.

Acknowledgments

We thank Y Watanabe (University of Tokyo) for critical reading of the manuscript. We also thank K Yokomori (UC Irvine) for providing the *SMC2* plasmid; D Trono (Swiss Federal Institute of Technology, Switzerland) for providing the lentiviral packaging and production plasmids psPAX2 and pMD2.G; H Miyoshi (Subteam for Manipulation of Cell Fate, RIKEN BioResource Center, Japan) and A Miyawaki (RIKEN Brain Science Institute, Japan) for providing the CSII-CMV-RfA-IRES2-Venus and CSII-CMV-Venus vectors; KJ Wu (National Yang Ming University) and M Fujii (Aichi Cancer Center) for providing plasmids; the Cell Bank of RIKEN BioResource Center (Japan), the Health Science Research Resource Bank (Japan), JCRB (Japan), ATCC, M Schwab (German Cancer Research Center [DKFZ]), and H Chiba (Fukushima Medical University) for providing cells; F Ohka and K Katsushima (Aichi Cancer Center Research Institute) for technical support for the GO analysis; MS Jackson and M Lastowska (Institute of Human Genetics, New Castle University) for providing the survival data of GSE13136; and the Children's Oncology Group, Children's Hospital of Philadelphia, University of Pennsylvania for clinical and outcome data. We thank M Foiani, F d'Adda di Fagagna, S Minucchi, and C-F Cheok (IFOM, Italy) for communicating unpublished results, and all members of our laboratory for their support and discussions. This work was funded in part by a grant from the Global COE Program (Integrated functional molecular medicine for neuronal and neoplastic disorders) to Nagoya University Graduate School of Medicine, a grant-in-aid from the National Cancer Center Research and Development Fund (22-4 to K.K.) and a Grant-in-Aid from the Ministry of Education, Culture, Sports, Science and Technology (MEXT), Japan (No. 24590376 to Y.M.-T. and No. 23110002 and 20390092 to K.K.).

Author Contributions

Y.M.-T., H.M., and K.K. conceived the project. Y.M.-T. performed most of the experimental procedures and analyzed the data. I.T. performed the statistical analysis. Y.K. and K.S. performed RNA-seq. J.-M.M. provided the prognosis data of the neuroblastoma patients. S.K. and H.I. performed the expression array of *MYCN*-Tg mice. Y.K. helped the data analysis of RNA-seq. Y.S. analyzed the data. Y.M.-T. and H.M. wrote the manuscript. K.K. supervised the project.

Supplemental Materials

Supplemental materials may be found here:
www.landesbioscience.com/journals/cc/article/27983

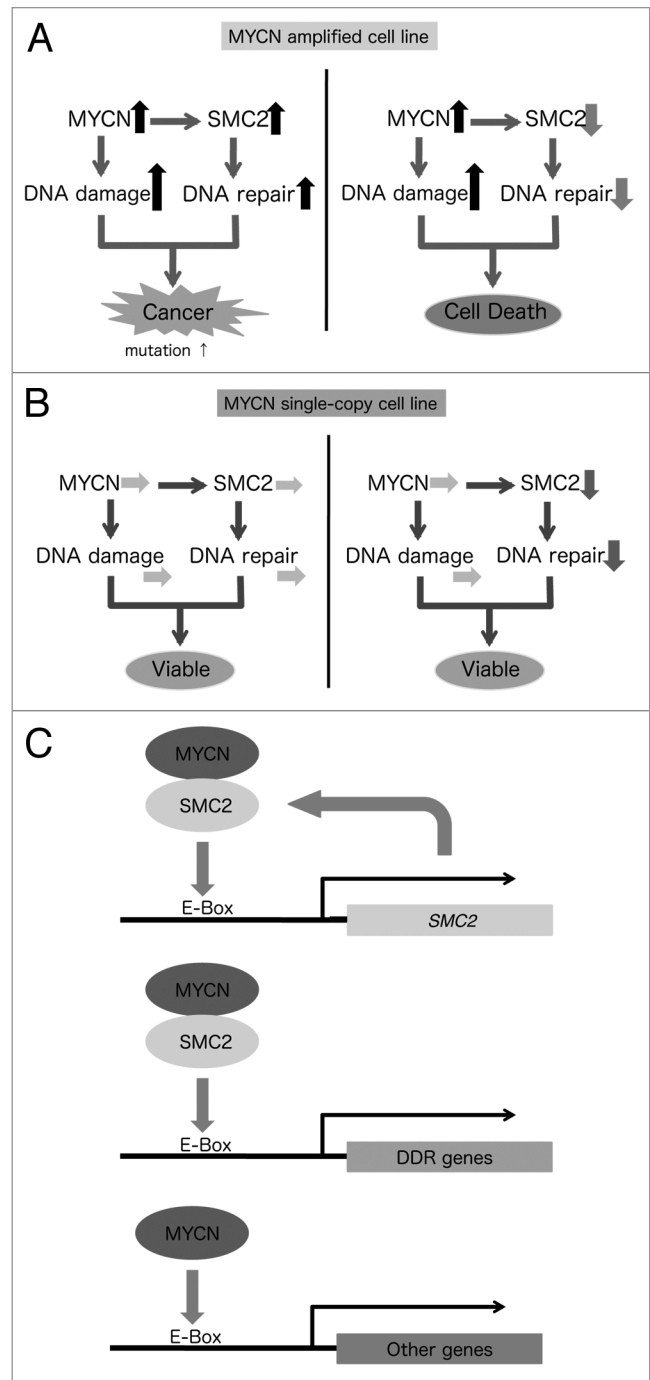


Figure 6. Schematic model showing the synergistic effects of SMC2 and MYCN in *MYCN*-amplified (A) and *MYCN* single copy (B) cells. This model is based on the proposed transcriptional regulation by MYCN and SMC2 (C).

References

- Hirano T. Condensins: universal organizers of chromosomes with diverse functions. *Genes Dev* 2012; 26:1659-78; PMID:22855829; <http://dx.doi.org/10.1101/gad.194746.112>
- Heale JT, Ball AR Jr., Schmiesing JA, Kim JS, Kong X, Zhou S, Hudson DF, Earnshaw WC, Yokomori K. Condensin I interacts with the PARP-1-XRCC1 complex and functions in DNA single-strand break repair. *Mol Cell* 2006; 21:837-48; PMID:16543152; <http://dx.doi.org/10.1016/j.molcel.2006.01.036>
- Aono N, Sutani T, Tomonaga T, Mochida S, Yanagida M. Cnd2 has dual roles in mitotic condensation and interphase. *Nature* 2002; 417:197-202; PMID:12000964; <http://dx.doi.org/10.1038/417197a>
- Akai Y, Kurokawa Y, Nakazawa N, Tonami-Murakami Y, Suzuki Y, Yoshimura SH, Iwasaki H, Shiomiwa Y, Nakamura T, Shibata E, et al. Opposing role of condensin hinge against replication protein A in mitosis and interphase through promoting DNA annealing. *Open Biol* 2011; 1:110023; PMID:22645654; <http://dx.doi.org/10.1098/rsob.110023>
- Xu Y, Leung CG, Lee DC, Kennedy BK, Crispino JD. MTB, the murine homolog of condensin II subunit CAP-G2, represses transcription and promotes erythroid cell differentiation. *Leukemia: official journal of the Leukemia Society of America. Leukemia Research Fund, UK* 2006; 20:1261-9; <http://dx.doi.org/10.1038/sj.leu.2404252>
- D'Ambrosio C, Schmidt CK, Katou Y, Kelly G, Itoh T, Shirahige K, Uhlmann F. Identification of cis-acting sites for condensin loading onto budding yeast chromosomes. *Genes Dev* 2008; 22:2215-27; PMID:18708580; <http://dx.doi.org/10.1101/gad.1675708>
- Fazio TG, Panning B. Condensin complexes regulate mitotic progression and interphase chromatin structure in embryonic stem cells. *J Cell Biol* 2010; 188:491-503; PMID:20176923; <http://dx.doi.org/10.1083/jcb.200908026>
- Menssen A, Hermeking H. Characterization of the c-MYC-regulated transcriptome by SAGE: identification and analysis of c-MYC target genes. *Proc Natl Acad Sci U S A* 2002; 99:6274-9; PMID:11983916; <http://dx.doi.org/10.1073/pnas.082005599>
- Fernandez PC, Frank SR, Wang L, Schroeder M, Liu S, Greene J, Cocito A, Amati B. Genomic targets of the human c-Myc protein. *Genes Dev* 2003; 17:1115-29; PMID:12695333; <http://dx.doi.org/10.1101/gad.1067003>
- Li Z, Van Calcar S, Qu C, Cavenee WK, Zhang MQ, Ren B. A global transcriptional regulatory role for c-Myc in Burkitt's lymphoma cells. *Proc Natl Acad Sci U S A* 2003; 100:8164-9; PMID:12808131; <http://dx.doi.org/10.1073/pnas.1332764100>
- Chiang YC, Teng SC, Su YN, Hsieh FJ, Wu KJ. c-Myc directly regulates the transcription of the NBS1 gene involved in DNA double-strand break repair. *J Biol Chem* 2003; 278:19286-91; PMID:12637527; <http://dx.doi.org/10.1074/jbc.M212043200>
- Perini G, Diolaiti D, Porro A, Della Valle G. In vivo transcriptional regulation of N-Myc target genes is controlled by E-box methylation. *Proc Natl Acad Sci U S A* 2005; 102:12117-22; PMID:16093321; <http://dx.doi.org/10.1073/pnas.0409097102>
- Luo J, Solimini NL, Elledge SJ. Principles of cancer therapy: oncogene and non-oncogene addiction. *Cell* 2009; 136:823-37; PMID:19269363; <http://dx.doi.org/10.1016/j.cell.2009.02.024>
- Halazonetis TD, Gorgoulis VG, Bartek J. An oncogene-induced DNA damage model for cancer development. *Science* 2008; 319:1352-5; PMID:18323444; <http://dx.doi.org/10.1126/science.1140735>
- Vafa O, Wade M, Kern S, Beeche M, Pandita TK, Hampton GM, Wahl GM. c-Myc can induce DNA damage, increase reactive oxygen species, and mitigate p53 function: a mechanism for oncogene-induced genetic instability. *Mol Cell* 2002; 9:1031-44; PMID:12049739; [http://dx.doi.org/10.1016/S1097-2765\(02\)00520-8](http://dx.doi.org/10.1016/S1097-2765(02)00520-8)
- Herold S, Herkert B, Eilers M. Facilitating replication under stress: an oncogenic function of MYC? *Nat Rev Cancer* 2009; 9:441-4; PMID:19461668; <http://dx.doi.org/10.1038/nrc2640>
- Polo SE, Jackson SP. Dynamics of DNA damage response proteins at DNA breaks: a focus on protein modifications. *Genes Dev* 2011; 25:409-33; PMID:21363960; <http://dx.doi.org/10.1101/gad.2021311>
- Chapman JR, Taylor MR, Boulton SJ. Playing the end game: DNA double-strand break repair pathway choice. *Mol Cell* 2012; 47:497-510; PMID:22920291; <http://dx.doi.org/10.1016/j.molcel.2012.07.029>
- Kaelin WG Jr. The concept of synthetic lethality in the context of anticancer therapy. *Nat Rev Cancer* 2005; 5:689-98; PMID:16110319; <http://dx.doi.org/10.1038/nrc1691>
- Farmer H, McCabe N, Lord CJ, Tutt AN, Johnson DA, Richardson TB, Santarosa M, Dillon KJ, Hickson I, Knights C, et al. Targeting the DNA repair defect in BRCA mutant cells as a therapeutic strategy. *Nature* 2005; 434:917-21; PMID:15829967; <http://dx.doi.org/10.1038/nature03445>
- Bryant HE, Schultz N, Thomas HD, Parker KM, Flower D, Lopez E, Kyle S, Meuth M, Curtin NJ, Helleday T. Specific killing of BRCA2-deficient tumours with inhibitors of poly(ADP-ribose) polymerase. *Nature* 2005; 434:913-7; PMID:15829966; <http://dx.doi.org/10.1038/nature03443>
- Cole KA, Huggins J, Laquaglia M, Hulderman CE, Russell MR, Bosse K, Diskin SJ, Attiyeh EF, Sennett R, Norris G, et al. RNAi screen of the protein kinome identifies checkpoint kinase 1 (CHK1) as a therapeutic target in neuroblastoma. *Proc Natl Acad Sci U S A* 2011; 108:3336-41; PMID:21289283; <http://dx.doi.org/10.1073/pnas.1012351108>
- Höglund A, Strömvall K, Li Y, Forshell LP, Nilsson JA. Chk2 deficiency in Myc overexpressing lymphoma cells elicits a synergistic lethal response in combination with PARP inhibition. *Cell Cycle* 2011; 10:3598-607; PMID:22030621; <http://dx.doi.org/10.4161/cc.10.20.17887>
- Toyoshima M, Howie HL, Imakura M, Walsh RM, Annis JE, Chang AN, Frazier J, Chau BN, Loboda A, Linsley PS, et al. Functional genomics identifies therapeutic targets for MYC-driven cancer. *Proc Natl Acad Sci U S A* 2012; 109:9545-50; PMID:22623531; <http://dx.doi.org/10.1073/pnas.1121119109>
- Murga M, Campaner S, Lopez-Contreras AJ, Toledo LI, Soria R, Montaña MF, D'Artista L, Schleker T, Guerra C, Garcia E, et al. Exploiting oncogene-induced replicative stress for the selective killing of Myc-driven tumors. *Nat Struct Mol Biol* 2011; 18:1331-5; PMID:22120667; <http://dx.doi.org/10.1038/nsmb.2189>
- Molenaar JJ, Ebus ME, Geerts D, Koster J, Lamers F, Valentijn LJ, Westerhout EM, Versteeg R, Caron HN. Inactivation of CDK2 is synthetically lethal to MYCN over-expressing cancer cells. *Proc Natl Acad Sci U S A* 2009; 106:12968-73; PMID:19525400; <http://dx.doi.org/10.1073/pnas.0901418106>
- Otto T, Horn S, Brockmann M, Eilers U, Schüttrumpf L, Popov N, Kenney AM, Schulte JH, Beijersbergen R, Christiansen H, et al. Stabilization of N-Myc is a critical function of Aurora A in human neuroblastoma. *Cancer Cell* 2009; 15:67-78; PMID:19111882; <http://dx.doi.org/10.1016/j.ccr.2008.12.005>
- Beierle EA, Trujillo A, Nagaram A, Kurenova EV, Finch R, Ma X, Vella J, Cance WG, Golubovskaya VM. N-MYC regulates focal adhesion kinase expression in human neuroblastoma. *J Biol Chem* 2007; 282:12503-16; PMID:17327229; <http://dx.doi.org/10.1074/jbc.M701450200>
- Rottmann S, Wang Y, Nasoff M, Deveraux QL, Quon KC. A TRAIL receptor-dependent synthetic lethal relationship between MYC activation and GSK3beta/FBW7 loss of function. *Proc Natl Acad Sci U S A* 2005; 102:15195-200; PMID:16210249; <http://dx.doi.org/10.1073/pnas.0505114102>
- Kessler JD, Kahle KT, Sun T, Meerbrey KL, Schlabach MR, Schmitt EM, Skinner SO, Xu Q, Li MZ, Hartman ZC, et al. A SUMOylation-dependent transcriptional subprogram is required for Myc-driven tumorigenesis. *Science* 2012; 335:348-53; PMID:22157079; <http://dx.doi.org/10.1126/science.1212728>
- Wang Y, Engels IH, Knee DA, Nasoff M, Deveraux QL, Quon KC. Synthetic lethal targeting of MYC by activation of the DR5 death receptor pathway. *Cancer Cell* 2004; 5:501-12; PMID:15144957; [http://dx.doi.org/10.1016/S1535-6108\(04\)00113-8](http://dx.doi.org/10.1016/S1535-6108(04)00113-8)
- George RE, Sanda T, Hanna M, Fröhling S, Luther W 2nd, Zhang J, Ahn Y, Zhou W, London WB, McGrady P, et al. Activating mutations in ALK provide a therapeutic target in neuroblastoma. *Nature* 2008; 455:975-8; PMID:18923525; <http://dx.doi.org/10.1038/nature07397>
- Janoueix-Lerosey I, Lequin D, Brugières L, Ribeiro A, de Pontual L, Combaret V, Raynal V, Puisieux A, Schleiermacher G, Pierron G, et al. Somatic and germline activating mutations of the ALK kinase receptor in neuroblastoma. *Nature* 2008; 455:967-70; PMID:18923523; <http://dx.doi.org/10.1038/nature07398>
- Mossé YP, Laudenslager M, Longo L, Cole KA, Wood A, Attiyeh EF, Laquaglia MJ, Sennett R, Lynch JE, Perri P, et al. Identification of ALK as a major familial neuroblastoma predisposition gene. *Nature* 2008; 455:930-5; PMID:18724359; <http://dx.doi.org/10.1038/nature07261>
- Chen Y, Takita J, Choi YL, Kato M, Ohira M, Sanada M, Wang L, Soda M, Kikuchi A, Igarashi T, et al. Oncogenic mutations of ALK kinase in neuroblastoma. *Nature* 2008; 455:971-4; PMID:18923524; <http://dx.doi.org/10.1038/nature07399>
- Maris JM, Hogarty MD, Bagatell R, Cohn SL. Neuroblastoma. *Lancet* 2007; 369:2106-20; PMID:17586306; [http://dx.doi.org/10.1016/S0140-6736\(07\)60983-0](http://dx.doi.org/10.1016/S0140-6736(07)60983-0)
- Cheung N-KV, Dyer MA. Neuroblastoma: developmental biology, cancer genomics and immunotherapy. *Nat Rev Cancer* 2013; 13:397-411; PMID:23702928; <http://dx.doi.org/10.1038/nrc3526>
- Weiss WA, Aldape K, Mohapatra G, Feuerstein BG, Bishop JM. Targeted expression of MYCN causes neuroblastoma in transgenic mice. *EMBO J* 1997; 16:2985-95; PMID:9214616; <http://dx.doi.org/10.1093/emboj/16.11.2985>
- Hansford LM, Thomas WD, Keating JM, Burkhardt CA, Peaston AE, Norris MD, Haber M, Armati PJ, Weiss WA, Marshall GM. Mechanisms of embryonal tumor initiation: distinct roles for MycN expression and MYCN amplification. *Proc Natl Acad Sci U S A* 2004; 101:12664-9; PMID:15314226; <http://dx.doi.org/10.1073/pnas.0401083101>
- Blackwell TK, Huang J, Ma A, Kretzner L, Alt FW, Eisenman RN, Weintraub H. Binding of myc proteins to canonical and noncanonical DNA sequences. *Mol Cell Biol* 1993; 13:5216-24; PMID:8395000
- Stracker TH, Petriani JH. The MRE11 complex: starting from the ends. *Nat Rev Mol Cell Biol* 2011; 12:90-103; PMID:21252998; <http://dx.doi.org/10.1038/nrm3047>

42. Bonner WM, Redon CE, Dickey JS, Nakamura AJ, Sedelnikova OA, Solier S, Pommier Y. GammaH2AX and cancer. *Nat Rev Cancer* 2008; 8:957-67; PMID:19005492; <http://dx.doi.org/10.1038/nrc2523>
43. Basu A, Krishnamurthy S. Cellular responses to Cisplatin-induced DNA damage. *J Nucleic Acids* 2010; 2010; PMID:20811617; <http://dx.doi.org/10.4061/2010/201367>
44. Shao RG, Cao CX, Zhang H, Kohn KW, Wold MS, Pommier Y. Replication-mediated DNA damage by camptothecin induces phosphorylation of RPA by DNA-dependent protein kinase and dissociates RPA:DNA-PK complexes. *EMBO J* 1999; 18:1397-406; PMID:10064605; <http://dx.doi.org/10.1093/emboj/18.5.1397>
45. Huang S, Laoukili J, Epping MT, Koster J, Hölzel M, Westerman BA, Nijkamp W, Hata A, Asgharzadeh S, Seeger RC, et al. ZNF423 is critically required for retinoic acid-induced differentiation and is a marker of neuroblastoma outcome. *Cancer Cell* 2009; 15:328-40; PMID:19345331; <http://dx.doi.org/10.1016/j.ccr.2009.02.023>
46. Wang Q, Diskin S, Rappaport E, Attiyeh E, Mosse Y, Shue D, Seiser E, Jagannathan J, Shusterman S, Bansal M, et al. Integrative genomics identifies distinct molecular classes of neuroblastoma and shows that multiple genes are targeted by regional alterations in DNA copy number. *Cancer Res* 2006; 66:6050-62; PMID:16778177; <http://dx.doi.org/10.1158/0008-5472.CAN-05-4618>
47. Łastowska M, Viprey V, Santibanez-Koref M, Wappler I, Peters H, Cullinane C, Roberts P, Hall AG, Tweddle DA, Pearson AD, et al. Identification of candidate genes involved in neuroblastoma progression by combining genomic and expression microarrays with survival data. *Oncogene* 2007; 26:7432-44; PMID:17533364; <http://dx.doi.org/10.1038/sj.onc.1210552>
48. Choi SH, Wright JB, Gerber SA, Cole MD. Myc protein is stabilized by suppression of a novel E3 ligase complex in cancer cells. *Genes Dev* 2010; 24:1236-41; PMID:20551172; <http://dx.doi.org/10.1101/gad.1920310>
49. Molenaar JJ, Koster J, Zwijnenburg DA, van Sluis P, Valentijn LJ, van der Ploeg I, Hamdi M, van Nes J, Westerman BA, van Arkel J, et al. Sequencing of neuroblastoma identifies chromothripsis and defects in neurogenesis genes. *Nature* 2012; 483:589-93; PMID:22367537; <http://dx.doi.org/10.1038/nature10910>
50. Mönnich M, Banks S, Eccles M, Dickinson E, Horsfield J. Expression of cohesin and condensin genes during zebrafish development supports a non-proliferative role for cohesin. *Gene Expr Patterns* 2009; 9:586-94; PMID:19723591; <http://dx.doi.org/10.1016/j.gep.2009.08.004>
51. Marchal JA, Ghani M, Schindler D, Gavvovidis I, Winkler T, Esquitino V, Sternberg N, Busche A, Krawitz P, Hecht J, et al. Misregulation of mitotic chromosome segregation in a new type of autosomal recessive primary microcephaly. *Cell Cycle* 2011; 10:2967-77; PMID:21857152; <http://dx.doi.org/10.4161/cc.10.17.16871>
52. Chen ES, Sutani T, Yanagida M. Cti1/C1D interacts with condensin SMC hinge and supports the DNA repair function of condensin. *Proc Natl Acad Sci U S A* 2004; 101:8078-83; PMID:15148393; <http://dx.doi.org/10.1073/pnas.0307976101>
53. Przewloka MR, Pardington PE, Yannone SM, Chen DJ, Cary RB. In vitro and in vivo interactions of DNA ligase IV with a subunit of the condensin complex. *Mol Biol Cell* 2003; 14:685-97; PMID:12589063; <http://dx.doi.org/10.1091/mbc.E01-11-0117>
54. Dávalos V, Suárez-López L, Castaño J, Messent A, Abasolo I, Fernandez Y, Guerra-Moreno A, Espín E, Armengol M, Musulen E, et al. Human SMC2 protein, a core subunit of human condensin complex, is a novel transcriptional target of the WNT signaling pathway and a new therapeutic target. *J Biol Chem* 2012; 287:43472-81; PMID:23095742; <http://dx.doi.org/10.1074/jbc.M112.428466>
55. Malynn BA, de Alboran IM, O'Hagan RC, Bronson R, Davidson L, DePinho RA, Alt FW. N-myc can functionally replace c-myc in murine development, cellular growth, and differentiation. *Genes Dev* 2000; 14:1390-9; PMID:10837031
56. Westermann F, Muth D, Benner A, Bauer T, Henrich KO, Oberthuer A, Brors B, Beissbarth T, Vandesompele J, Pattyn F, et al. Distinct transcriptional MYCN/c-MYC activities are associated with spontaneous regression or malignant progression in neuroblastomas. *Genome Biol* 2008; 9:R150; PMID:18851746; <http://dx.doi.org/10.1186/gb-2008-9-10-r150>
57. Miyoshi H, Takahashi M, Gage FH, Verma IM. Stable and efficient gene transfer into the retina using an HIV-based lentiviral vector. *Proc Natl Acad Sci U S A* 1997; 94:10319-23; PMID:9294208; <http://dx.doi.org/10.1073/pnas.94.19.10319>
58. Miyoshi H, Blömer U, Takahashi M, Gage FH, Verma IM. Development of a self-inactivating lentivirus vector. *J Virol* 1998; 72:8150-7; PMID:9733856
59. Wang K, Diskin SJ, Zhang H, Attiyeh EF, Winter C, Hou C, Schnepf RW, Diamond M, Bosse K, Mayes PA, et al. Integrative genomics identifies LMO1 as a neuroblastoma oncogene. *Nature* 2011; 469:216-20; PMID:21124317; <http://dx.doi.org/10.1038/nature09609>